Final version at http://ecst.ecsdl.org/content/72/1/3.abstract

Towards Additive Manufacturing of Tungsten Carbide Using Renewable Resources

M. Islam[a] and R. Martinez-Duarte[a]

[a] Department of Mechanical Engineering, Clemson University, Clemson, South Carolina 29634, USA

Here we present preliminary results towards additive manufacturing of carbides. A biopolymer-metal oxide gel composite composed of iota-carrageenan, chitin and tungsten trioxide (WO_3) was shaped and heat treated in order to obtain carbide structures. Upon heat treatment of this composite above 900 °C, a porous structure of tungsten carbide (WC) was obtained. The synthesis mechanism of WC was estimated using the result from XRD characterization. The synthesized WC was characterized with SEM, TEM and nitrogen absorption-desorption to investigate the morphology, particle size and pore size distribution. The carbonaceous materials retained the original shape. The ongoing work is on studying the rheology of the gel composites to extrude through additive manufacturing system to obtained 3D printed carbide parts.

Introduction

Carbides are one of the most interesting groups of materials because they show unique properties such as high chemical stability, low thermal expansion, high thermal conductivity and high temperature resistance. Among the several carbide synthesis methods, carbothermal reduction reaction is the most preferred technique in industries as it allows to use a wide range of material as precursor [1]. In a carbothermal reaction, a metal oxide nanoparticle is reduced to metallic element in the presence of carbon through heat treatment in an inert atmosphere. Such metallic element then reacts with the carbon excess to form its carbide [2].

Additive manufacturing (AM) is a fast-emerging technology in which a shape is fabricated using layer-by-layer deposition of a material, in a bottom up manufacturing operation. AM technology allows for the fabrication of 3D parts with complex geometrical features that are difficult to manufacture using traditional machining techniques [3]. Examples of such geometrical features include turbine wheels [4] and porous honeycomb structures for particulate filters in the exhaust of automobile engines [5]. In recent years, the extrusion of pastes in AM have become popular for applications ranging from tissue engineering to food manufacturing [6,7]. The choice of materials is wide and in particular includes materials such as photo-crosslinkable hydrogels [8], gelatin [9], collagen [10] and alginate hydrogel [11].

Here we report initial results towards the additive manufacturing of carbides using paste-like precursors. We use a biopolymer-metal oxide composite as a precursor to

obtain carbide. This composite exhibits Bingham plastic behavior, it only yields after a specific stress value, which allows for its extrusion into shapes at room temperature. Upon heat treatment in an inert atmosphere, the biopolymer carbonizes at 900 °C. Further increase in the temperature leads to the carbothermal reduction of the metal oxide and eventually to the formation of carbide. Hence, carbides can be obtained in a route that has the potential to be more energy-efficient than current processes. The use of renewable biopolymers as the carbon source enables the elimination of petroleum-based precursors and the colloidal dispersion of oxide nanoparticles in the polymer, which eventually transforms to carbon, matrix allows for a proximity between reagents that reduces the temperature necessary for a carbide-forming reaction. In this work we focus on the synthesis of tungsten carbide from a composite featuring iota-carrageenan and chitin as the biopolymer matrix and tungsten trioxide as the metal oxide. We characterize the impact of process temperature in the composition of the material.

Materials and Methods

Materials

The biopolymer gel used in this work consists of two biopolymers: iota-carrageenan (IC) and chitin. IC was used as a carrier material as it forms a Bingham plastic while dissolved in aqueous solution. The role of chitin was to fill the gel network formed by the carrier material. IC and chitin were purchased from Sigma Aldrich, USA and used as purchased. High purity tungsten trioxide (WO_3) nanoparticles featuring 25-65 nm (US Research Nanomaterials Inc., USA) diameter were used as purchased. Ultra-pure water was used for the preparation of gel composite.

Experimental Procedure

IC and chitin powders were mixed in the dry in a weight ratio of 1:4. WO_3 nanoparticles were then added to the mixture using a vortex mixer (Thermo Scientific, Maximix M16710-33Q) for 10 minutes to obtain an molar ratio of WO_3:C ratio as 1:6. Such ratio was calculated based on the carbon yield (8%) from IC and chitin mixture obtained through thermogravimetric analysis (data not shown). Ultra-pure water was then added to such dry mixture and stirred thoroughly to achieve a gel composite. The gel composite was loaded into a 5 ml syringe and manually extruded to form a spiral shape, ~ 10 mm-tall, on an alumina substrate (Kyocera, Japan).

The extruded composite was heat treated at different final temperatures ranging from 750 °C to 1450° C in a tube furnace (for temperature < 1400 °C, model TF1400; temperature > 1400 °C, model TF1700, Across International, USA) under a constant nitrogen gas flow rate of 10 SCFH (Standard Cubic Feet per Hour). The heating protocol consisted of 5 steps: (a) room temperature to 300 °C with a heating ramp of 5 °C/min; (b) a dwell at 300 °C for 30 minutes to eliminate the excess oxygen from the furnace tube; (c) from 300 °C to final temperature with 5 °C/min temperature ramp; (d) dwell at the final temperature for 3 hours and finally (e) natural cooling to room temperature by turning off the furnace.

Characterization

X-ray diffraction (XRD) spectroscopy using Cu-Kα radiation (Rigaku Ultima IV, Japan) was performed to determine the crystallinity and composition of the heat treated samples. The morphology of the heat treated samples was characterized by scanning electron microscopy (SEM, Hitachi SU6600, Japan). The elemental analysis of the samples was also carried out by energy dispersed X-ray spectroscopy (EDX, Oxford Instruments, USA) mounted on the SEM. High resolution transmission electron microscopy (HRTEM) analysis was performed using a H9500 (Hitachi, Japan) electron microscope with an acceleration voltage of 200 kV. The TEM sample was prepared using a focused ion beam (FIB) milling machine (NB5000, Hitachi, Japan). The pore size distribution was characterized by nitrogen adsorption-desorption using Quantachrome Autosorb iQ gas sorption analyser (Quantachorme Instruments, USA).

Results and Discussions

The crystallographic composition obtained with XRD analysis for all samples is presented in Fig. 1a. The XRD patterns were indexed with hexagonal tungsten carbide (WC), that matches with the International Centre of Diffraction Data (ICDD) PDF number 01-072-0097. At 750°C and 900 °C, no formation of tungsten carbide was observed. At 750 °C, the peaks were indexed to WO_3 and $W_{18}O_{49}$, wherein peaks for only metallic tungsten (W) were obtained at 900 °C. Peaks for WC were observed at 960 °C along with the hemicarbide (W_2C) and the metallic tungsten (W). The intensity of the peaks for WC increases with an increase in temperature, whereas the intensities of the peaks for W_2C and W decrease. At 1450 °C, WC becomes the dominant material with a weak presence of W_2C.

The XRD data supports the following theory of tungsten carbide formation. Upon heat treatment of the gel composite, IC and chitin turn into a carbon rich product in the temperature range 350-600 °C [12]. At this stage, the WO_3 nanoparticles are expected to be surrounded by a highly porous carbon matrix. In the presence of carbon, WO_3 is reduced to W at a temperature higher than 750 °C [13,14]. Other compositions such as WO_{3-x} and WO_2 are also formed during the reduction of WO_3 to W. The oxygen particles of the WO_3 react with the surrounding carbon to form carbon monoxide (CO) and carbon dioxide (CO_2) during the reduction of WO_3 to W. Upon complete reduction of WO_3, the resultant W reacts with the carbon at higher temperature to form WC. The following reactions are expected to occur during the whole process [15]:

$$WO_3 + C \rightarrow WO_2 + CO \quad [1]$$

$$WO_2 + 2CO \rightarrow W + 2CO_2 \quad [2]$$

$$CO_2 + 2C \rightarrow 2CO \quad [3]$$

$$W + C \rightarrow WC \quad [4]$$

I_n/I_{total} was plotted against the reaction temperature to estimate the relative presence of WC, W_2C and W in the carbonaceous material as presented in Figure 1b. Here I_n represents the sum of the peak intensities corresponding to a particular phase and I_{total} stands for the sum of all the peak intensities present in the XRD pattern. Clearly, the proportional amount of WC increases with an increase in the reaction temperature,

whereas the proportional amount of W_2C and W decreases. An increase in the reaction temperature improves the solid-solid reaction of W and surrounding carbon that leads to WC formation. Also, the phase transformation from W_2C to WC occurs with increasing temperature. At 1450 °C, relative amount of W decreases down to zero, which ensures the complete carburization of W. A small amount of W_2C is still present in the sample. We assume that the present W_2C can be carburized further into WC at higher temperature with WC being the sole material present in the sample [16].

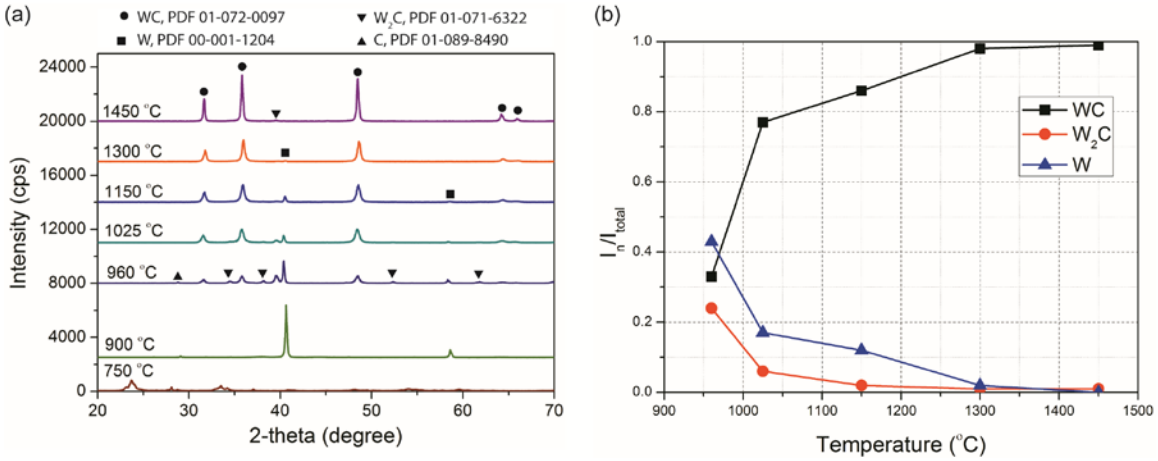

Figure 1: (a) XRD pattern of carbonaceous material obtained from heat treatment of IC-Chitin-WO_3 composite at different temperature; (b) Plot of I_n/I_{total} against the reaction temperature.

Further characterization of composition, grain size and porosity was conducted with the samples obtained at 1300 °C. The results obtained with SEM characterization are shown in Figure 2a. An agglomerate of particles can be clearly seen. EDX of the sample (not shown here) confirmed the presence of W and C in the material in a W:C molar ratio of 1, which also confirms the synthesis of WC. HRTEM analysis was then conducted, and its results shown in Figure 2b. The WC obtained in this procedure features a grain size of 30-50 nm. Lattice fringes shown in the Figure 2b have a *d* spacing of 2.525 Å, which attributes to the (100) plane of hexagonal WC. This also confirms the formation of WC in this process. It should be noted that the WC synthesized here is porous. Tiny pores can be seen in the SEM images as indicated by arrows in Figure 2a. The nitrogen adsorption-desorption isotherm shown in Figure 2c also indicates the formation of mesopores (2-50 nm) in the sample. Our hypothesis is that the escape of water from the material at the very beginning leads to the porosity between grains while the escape of gaseous material during carbonization and carbide synthesis results in the pores in the material. The inter grain pore size is 10-50 nm as measured from the SEM images The plot for the material pore size distribution (inset of Figure 2c) shows that the average pore size in the material is around 18 Å. The total pore volume was measured to be 6.34 X 10^{-2} cm^3/g.

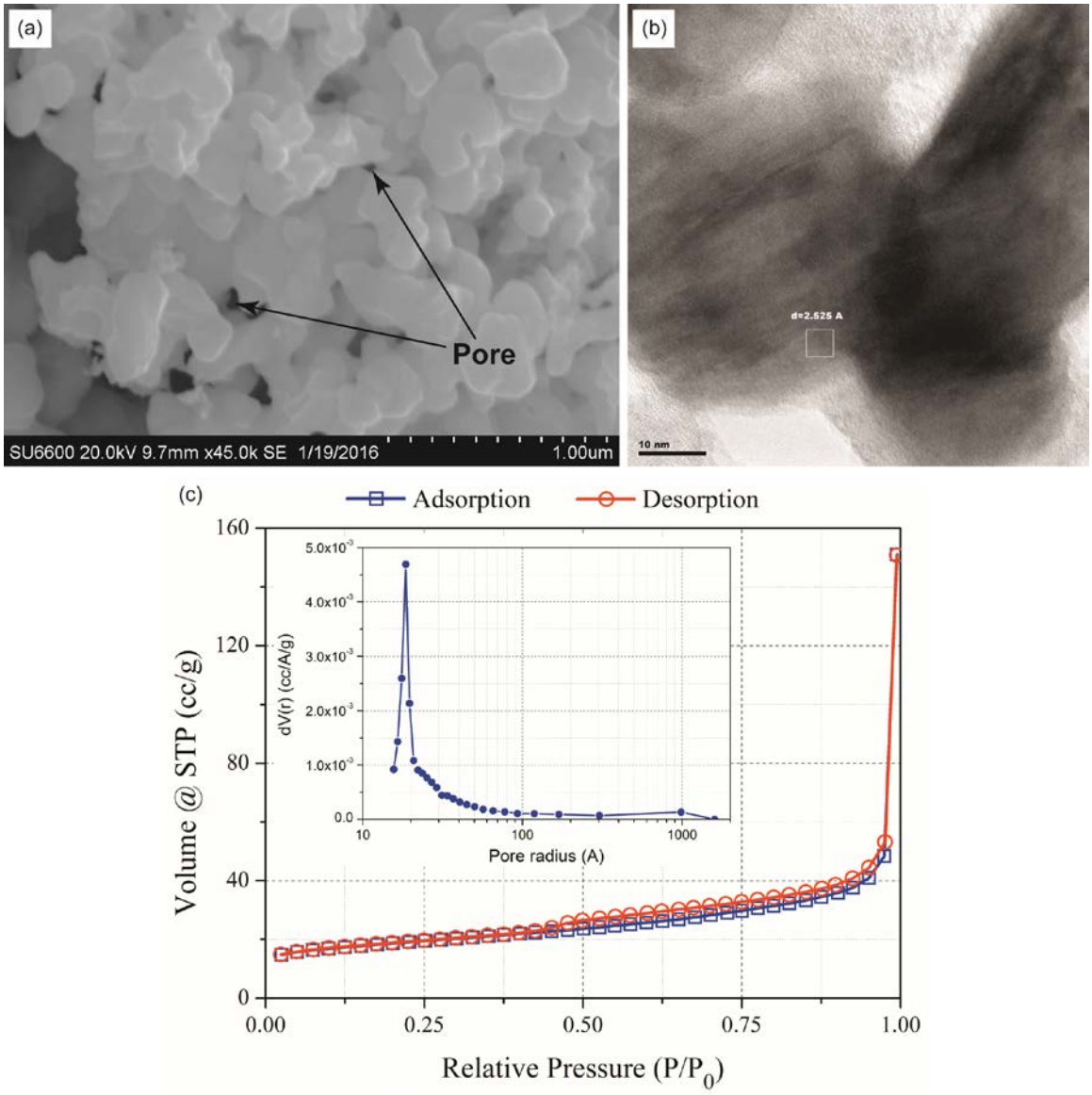

Figure 2: (a) SEM image of the carbonaceous material obtained from the heat treatment of the gel composite at 1300 °C; (b) HRTEM image of the WC material obtained at 1300 °C; (c) Nitrogen adsorption-desorption isotherm and pore size distribution (inset) for the WC synthesized at 1300 °C.

Conclusion

Here we present the use of a biopolymer-metal oxide composite as precursor of tungsten carbide. We heat treated an extruded composite featuring iota-carrageenan, chitin and WO_3. Optimization of the heat treatment protocol leads to the derivation of a porous Tungsten carbide (WC) at 1450 °C. The grain size of the material is between 30-50 nm with inter-grain porosity of 10-50 nm. The average pore size in the material itself was around 18 Å. These characteristics are similar to current WC materials [17]. The process temperature of 1450 °C compares advantageously to current WC processing temperatures of 1600-2000 °C [18].

The elimination of petroleum-based carbon precursors also reflects a more environmental-friendly approach. In the United States alone, carbon black production is estimated to be around 2 million metric tons/year, consuming around 450 million gallons of oil [19,20]. As mentioned earlier, the biopolymers used in this work are renewable. Iota-carrageenan is a sulfated polysaccharide extracted from seaweed and widely used in the food industry as a thickener and additive. Iota-carrageenan is extracted from natural or farmed *Eucheuma spinosum*, in Indonesia, the Philippines, and the United Republic of Tanzania with positive socio-economic implications [21]. Chitin is another abundant biopolymer. The principal source of chitin is the exoskeleton of shellfish such as shrimp, crab and lobster [22]. The total annual production of shrimp is reported to be 6 million ton per year in shrimp firming [23]. As the production of shrimp increases in firming, the utilization of its waste products is becoming increasingly important [24].

Ongoing work is on the extrusion of different composite formulations using a Fused Deposition Modeling (FDM) 3D printer and characterizing the impact of process parameters, such as extrusion rate, head velocity and nozzle size, on the reproducibility of dimensions, composition and porosity of complex shapes.

Acknowledgments

The authors are thankful to several Clemson colleagues: Dr. Laxmikant Saraf and Dr. Taghi Darroudi from the Electron Microscopy Facility for invaluable help regarding SEM/EDX and TEM analysis, Dr. Colin McMillen from the Structure Centre for XRD analysis and Prof. Stephen Creager and Jamie Shetzline for facilitating pore size distribution analysis.

References

1. A. Devečerski et al., *Process. Appl. Ceram.*, **5**, 63–67 (2011).
2. J. Barker, M. Y. Saidi, and J. L. Swoyer, *J. Electrochem. Soc.*, **150**, A684 (2003) http://jes.ecsdl.org/cgi/doi/10.1149/1.1568936.
3. N. Guo and M. C. Leu, *Front. Mech. Eng.*, **8**, 215–243 (2013).
4. T. Friedel, N. Travitzky, F. Niebling, M. Scheffler, and P. Greil, *J. Eur. Ceram. Soc.*, **25**, 193–197 (2005).
5. K. Naruse and K. Tajima, (2008).
6. F. P. W. Melchels et al., *Prog. Polym. Sci.*, **37**, 1079–1104 (2012).
7. J. Yang, L. W. Wu, and J. Liu, **1** (2001).
8. Y. Lu, G. Mapili, G. Suhali, S. Chen, and K. Roy, *J. Biomed. Mater. Res. A*, **77**, 396–405 (2006).
9. X. Wang et al., *Tissue Eng.*, **12**, 83–90 (2006).
10. R. L. Stewart et al., *Tissue Eng.*, **10**, 1566–1576 (2004).
11. S. Khalil and W. Sun, *J. Biomech. Eng.*, **131**, 111002 (2009).
12. M. Sevilla and A. B. Fuertes, *Chem. - A Eur. J.*, **15**, 4195–4203 (2009).
13. G. Leclercq et al., *J. Catal.*, **158**, 142–169 (1996).
14. D. S. Venables and M. E. Brown, *Thermochim. Acta*, **291**, 131–140 (1997).
15. P. Hoier, thesis, Chalmers University of Technology (2014).

16. R. Koc and S. K. Kodambaka, *J. Eur. Ceram. Soc.*, **20**, 1859–1869 (2000).
17. Z. Z. Fang, X. Wang, T. Ryu, K. S. Hwang, and H. Y. Sohn, *Int. J. Refract. Met. Hard Mater.*, **27**, 288–299 (2009).
18. SIDS, *Tungsten Carbide*, UNEP Publications, (2005).
19. T. A. Ruble, in *Refining Petroleum for Chemicals*,, p. 264–270, ACS Publication, Houston, TX (1970).
20. N. Z. Muradov and T. N. Veziroğlu, *Int. J. Hydrogen Energy*, **30**, 225–237 (2005).
21. D. Valderrama, J. Cai, N. Hishamunda, and N. Ridler, *Social and economic dimensions of carrageenan seaweed farming: a global synthesis*, p. 5-59, (2013).
22. M. Rinaudo, *Prog. Polym. Sci.*, **31**, 603–632 (2006).
23. R. Gillett, *Fish. Bethesda*, **475**, 331 pp. (2008).
24. P. S. Barber, J. L'Shamshina, and R. D. Rogers, *Pure Appl. Chem.*, **85**, 1693–1701 (2013).